COBEM 2023 27TH INTERNATIONAL CONGRESS OF MECHANICAL ENGINEERING

ABCM Brazilian Society of Mechanical Sciences and Engineering
27th ABCM International Congress of Mechanical Engineering
December 04-08, 2023, Florianópolis-SC, Brazil

COB-2023-1292
Design of passive dynamic absorbers to attenuate pathological tremor of human upper limb

Gabriel Guimarães de Souza Braga de Albuquerque
Marcela Rodrigues Machado
Braion Barbosa de Moura
Department of Mechanical Engineering, University of Brasília, 70910-900, Brasília, Brazil.
gabriel.bsag@gmail.com,marcelam@unb.br,braionbarbosa@gmail.com

Abstract. *Tremors in the limbs are a common symptom in several neurodegenerative diseases such as Parkinson's Disease, which can cause social discomfort and difficulties performing everyday tasks. When considering the possibility of drug allergy, the degree of invasion of the treatment, and the efficiency of the treatment, it is inevitable the use of vibration-attenuating devices stands out from the others in combating tremors in the limbs. Thus, this study aims to investigate the best configuration of mechanical vibration absorbers in suppressing tremors in Parkinson's patients by varying the position and size of each absorber. Controller effectiveness will be analyzed regarding response magnitude and percentage of amplitude reduction in both frequency and time domains. Results indicate that using vibration-absorbing devices significantly reduces the tremor amplitude, and the best configuration was absorbers in parallel. Also, the effects of more than two absorbers in parallel along the forearm and the design of new absorbers designed to control human limb tremors are investigated. Analytical models of the arm and passive controls are used to estimate the arm's vibration characteristics and evaluate the efficiency of the controls under three levels of pathology tremor excitation.*

Keywords: *Dynamic Absorber, Passive Vibration Control, Parkinson Disease.*

1. INTRODUCTION

The human body can exhibit tremors characterized by a rhythmic oscillation of the limbs, which can lead to social discomfort and difficulty performing basic everyday tasks. While limb tremors can be easily observed in some cases, an accurate diagnosis requires careful investigation, as various conditions can manifest with this symptom, and treatment approaches may also vary considerably from one condition to another, as discussed in (Crawford III and Zimmerman, 2018). In human limbs is an increasingly present need in individuals with neurodegenerative diseases such as Parkinson's Disease, White Hand Syndrome, Essential Tremor and others (Chou, 2004). Generally, these diseases have a series of unpleasant symptoms. Also, there are some medications that can cause symptoms similar to those of Parkinsonism.

One of the most prominent is tremors in the upper limbs, occurring more frequently in the individual's fingers, hands and arms. In the context of Parkinson's diseases, tremors are defined by repetitive and involuntary oscillations in the limbs which usually initiates in upper limbs. They may occur, in a lasting way, in postural conditions (limb in a resting or static position), kinetic (limb in movement) or both (Crawford III and Zimmerman, 2018). The rest tremor of Parkinsonism is in the range between 3 and 7 Hz, whereas the postural tremor is in the range between 5 and 12 Hz as shown in Morrison et al. (2008). In addition, tremors can also be classified by frequency and amplitude of oscillations.

Some alternatives to treat those neurodegenerative diseases or to control the corresponding tremors are already being explored through drugs, surgery, electrical stimulation, light therapy, transcranial magnetic stimulation, orthoses and vibration attenuating devices. However, each alternative may present negative or impeding points, differing from one person to another (Diaz and Louis, 2010). Thus, when considering the possibility of drug allergy, the degree of invasion of the treatment and the efficiency of the treatment, it is inevitable the use of vibration attenuating devices stand out from the others in combating tremors in the limbs (Fromme et al., 2019).

To reduce the burden of this disease, a dynamic vibration absorber can be designed to suppress the undesirable motion. The dynamic vibration absorber (DVA) is a passive vibration controller added in a system to as part of a remedial course of action at a particular frequency. The parameters of it are chosen to minimize the amplitude, principally the vibration at an undesired frequency. The limb system behavior can be translated into the movements of masses. Hashemi et al. (2004) proposed a two degree-of-freedom (DOF) model of upper limb with mass concentrated at centroid and inertia. The human arm was shaped on the horizontal plane as two rigid segments to describe the arm musculature planar motion of elbow and shoulder joints, but motion at wrist joint was not included. Gebai et al. (2016a) improved the mass-spring model considering the human hand as a three DOF system by increasing the motion of the palm. Also, he added the motion transmitted to the palm and the wrist joint as well as the movements from the biceps.

In this paper, we analyse and compare the efficiency of different configurations of dual and triple passive dynamic

absorber controllers in minimizing vibration originated from an excitation of human upper limb structure by Parkinson's disease. The analytical models of the arm and passive controls approached in this paper follow the work of Gebai et al. (2016a), and study of the limber under three levels of pathology tremor excitation is performed. Results show the efficiency of the dynamic absorbers that could drastically attenuate the tremor. The present work represents an expansion of the research presented by Albuquerque et al. (2023).

2. HUMAN UPPER LIMB STRUCTURE

The analytical model of the upper limb used in the study follows the model presented by Gebai et al. (2016a) and Hosseini et al. (2021). It consists of three-degree-of-freedom biodynamic modelling that considers the flexion-extension planar motion in the horizontal plane at the shoulder, elbow and wrist joints. Figure 1(LHS) shows the human upper limb parts and Fig. 1(RHS) the model proposed by the authors. The active input moments producing motion are considered due to shoulder, biceps, elbow and wrist muscle activation operating at the problematic frequencies in the range of the resting tremor.

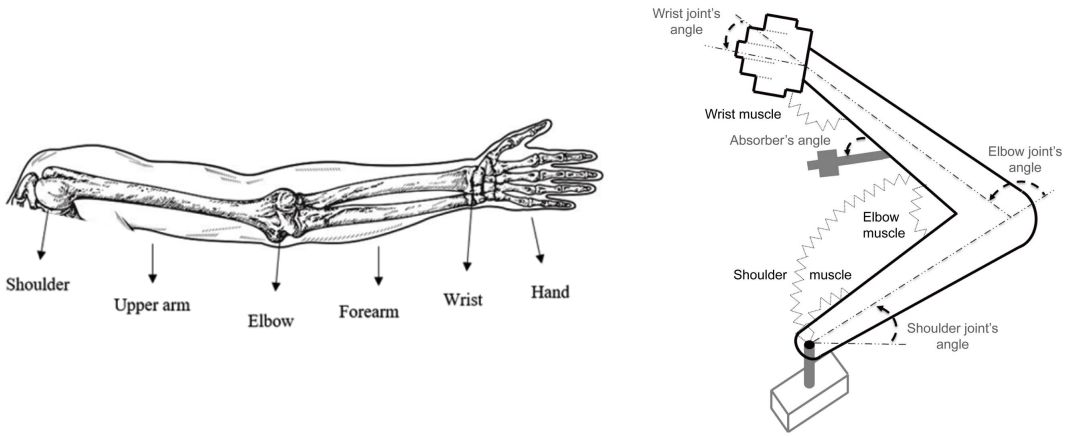

Figure 1: Schematic of a Human upper limb (LHS) and relation of the bio-mechanical model (RHS) by Gebai et al. (2018)

2.1 Mechanical upper limb design

The parameters of mass and inertia, as well as the length, mass, density and position of the centroid for the right hand, were calculated based on data provided experimentally by Contini (1972). The length of upper arm is represented by l_1, forearm by l_2, and palm by l_3, as shown in Fig. 2, and Table 2 contain the mass and inertia of each segment. The total mass of the considered system is $3.77\ kg$. The centroids are refereed in Fig. 2 as a_1 (upper arm), a_2 (forearm) and a_3 (palm), and inertia of the upper arm by I_1, the forearm by I_2, and the palm by I_3. Two configurations of dynamic vibration absorbers (DVA) are tested. The dual parallel absorbers (DPA) are settled at point B on ab_i, $i = \{2, 3\}$, position from point A (elbow), as shown in Fig. 2. The triple parallel absorbers (TPA) increase an absorber located on the upper arm at position ab_1 from the shoulder. The position from the absorber's mass to its joint along the beam is lab_i, $i = \{1, 2, 3\}$. In points b_i, $i = \{1, 2, 3\}$, the absorbers are considered with an additional mass of $m_d = 0.0522\ kg$ to increase the controller device (Gebai et al., 2016a). In the DPA and TPA, the total device mass is $0.44751\ kg$.

Table 1: The lenght and weight of each upper limb structure (Gebai et al., 2016a).

Right Hand	Length (cm)	Mass (kg)
Upper arm	36.4	2.070
Forearm	29.9	1.160
Palm	20.3	0.540

Table 2: Hand Arm Parameters (Gebai et al., 2016a).

Right Hand	Density (kg/m^3)	Centroid (m)	Moments of Inertia (kgm^2/rd)
Upper arm	1088.0	$0.427 \cdot l_1$	0.0228
Forearm	1108.6	$0.417 \cdot l_2$	0.0082
Palm	1112.6	$0.361 \cdot l_4$	0.0012

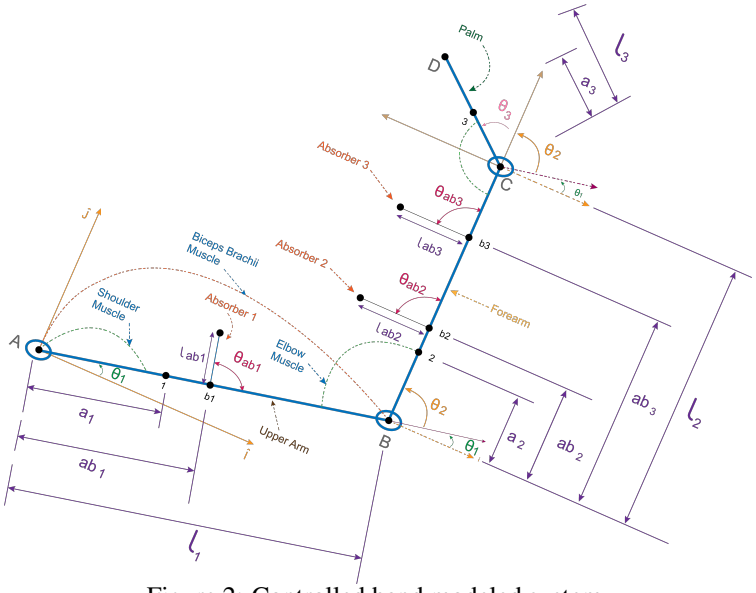

Figure 2: Controlled hand modeled system.

The Table 3 lists the stiffness values assumed at the shoulder's joint indicated by k_1, elbow as k_2, biceps as k_3, and wrist as k_4.

Table 3: Designed Parameters of Joint's Muscles (Gebai et al., 2016a)

Muscle	Stiffness coefficient (Nm/rd)	Damping coefficient (Nms/rd)
Shoulder	170	$0.002 \cdot k_1$
Elbow	150	$0.002 \cdot k_2$
Biceps	40	$0.002 \cdot k_3$
Wrist	10	$0.001 \cdot k_4$

3. Dynamic model of the upper limb

The dynamic model of the upper limb, named the principal system, consists of a three-DOF system. The motion will start at an instance of stability when $\theta_1 = 0^o$, $\theta_2 = 90^o$, and $\theta_a = 0^o$ with zero angular velocities as indicated in Fig. 2. The equation of motion follows Gebai et al. (2016b). The kinematics equations used Coriolis Theorem to obtain the three-DOF systems related to three angular displacements according to the global coordinate system, yields:

$$v_1 = v_A + \Omega_{xyz/XYZ} \times r_{1/A} = a_1\dot{\theta}_1\, j \tag{1}$$

$$v_B = v_A + \Omega_{xyz/XYZ} \times r_{B/A} = l_1\dot{\theta}_1\, j \tag{2}$$

$$v_2 = v_B + (v_{2/A}) + \Omega_{xyz/XYZ} \times r_{2/B} = -a_2(\dot{\theta}_1 + \dot{\theta}_2)\, i + l_1\dot{\theta}_1\, j \tag{3}$$

$$v_C = v_B + (v_{C/B}) + \Omega_{xyz/XYZ} \times r_{C/B} = -l_2(\dot{\theta}_1 + \dot{\theta}_2)\, i + l_1\dot{\theta}_1\, j \tag{4}$$

$$v_3 = v_C + (v_{3/C})_{x'y'z'} + \Omega_{x'y'z'/XYZ} \times r_{3/C} = -[(a_3 + l_2)(\dot{\theta}_1 + \dot{\theta}_2) + a_3\dot{\theta}_3]\, i + l_1\dot{\theta}_1\, j \tag{5}$$

Therefore, using the Lagrange equation, where the Rayleigh dissipation function is added to obtain the damping contribution, to form equations of motion for the systems will be:

$$\frac{d}{dt}\left(\frac{\partial T}{\partial \dot{q}_i} - \frac{\partial U}{\partial \dot{q}_i}\right) - \frac{\partial T}{\partial q_i} + \frac{\partial U}{\partial q_i} = F_i + F_{ci}\,, \qquad i = \{1, 2, 3\} \tag{6}$$

The Kinetic Energy is represented as

$$T = \left[\frac{1}{2}I_1\dot{\theta}_1^2 + \frac{1}{2}m_1v_1^2\right] + \left[\frac{1}{2}I_2(\dot{\theta}_1 + \dot{\theta}_2)^2 + \frac{1}{2}m_1v_1^2\right] + \left[\frac{1}{2}I_3\dot{\theta}_3^2 + \frac{1}{2}m_4v_4^2\right] \tag{7}$$

where each segment (upper arm, forearm and palm) was representing your portion in motion. The Potential Energy is of the form

$$U = \frac{1}{2}k_1\theta_1^2 + \frac{1}{2}k_2\theta_2^2 + \frac{1}{2}k_3(\theta_1 + \theta_2)^2 + \frac{1}{2}k_4\theta_3^2 \tag{8}$$

and Rayleigh dissipation function is represented by

$$C = \frac{1}{2}c_1\dot{\theta_1^2} + \frac{1}{2}c_2\dot{\theta_2^2} + \frac{1}{2}c_3(\dot{\theta_1} + \dot{\theta_2})^2 + \frac{1}{2}c_4\dot{\theta_3^2} \tag{9}$$

The generalized equation of motion has the form

$$\mathbf{M}\ddot{\theta} + \mathbf{C}\dot{\theta} + \mathbf{K}\theta = \mathbf{f} \tag{10}$$

where θ,$\dot{\theta}$, $\ddot{\theta}$ are the angular displacement, velocity and acceleration vectors at the hand joints, respectively. For the uncontrolled hand system, $\theta_{1,2,3}$ corresponds to the flexion angle at the shoulder, elbow and wrist joints, respectively. Hence, matrix are expressed as:

$$\mathbf{M} = \begin{bmatrix} M_{11} & M_{12} & M_{13} \\ M_{21} & M_{22} & M_{23} \\ M_{31} & M_{32} & M_{33} \end{bmatrix} \tag{11}$$

where,

$$\begin{aligned} M_{11} &= (I_1 + m_1a_1^2) + (I_2 + m_2a_2^2) + m_2l_1^2 + m_4(l_1^2 + l_2^2 + a_4^2 + 2l_2a_4) \\ M_{12} &= (I_2 + m_2a_2^2) + m_4(l_2^2 + a_4^2 + 2l_2a_4) \\ M_{13} &= m_4(a_4^2 + l_2a_4) \\ M_{21} &= M_{12} \quad M_{22} = M_{12} \quad M_{23} = M_{13} \\ M_{31} &= M_{13} \quad M_{32} = M_{23} \quad M_{33} = I_4 + m_4a_4^2 \end{aligned}$$

$$\mathbf{K} = \begin{bmatrix} k_1 + k_3 & k_3 & 0 \\ k_3 & k_2 + k_3 & 0 \\ 0 & 0 & k_4 \end{bmatrix} \tag{12}$$

$$\mathbf{C} = \begin{bmatrix} c_1 + c_3 & c_3 & 0 \\ c_3 & c_2 + c_3 & 0 \\ 0 & 0 & c_4 \end{bmatrix} \tag{13}$$

3.1 Excitation force

The force $f_{1,2,3}$ are the input moments due to shoulder, biceps, elbow and wrist muscle activation, respectively. Those moments are driven at the first three resonance frequencies of the primary system as a triple harmonic function representing the resting tremor.

$$\mathbf{f^T} = \begin{bmatrix} f_1 & f_2 & f_3 \end{bmatrix}^T$$

$$\mathbf{f}_{1,2,3} = 1\cos(\omega_1 t) + 1\cos(\omega_2 t) + 1\cos(\omega_3 t), \qquad \text{for} \quad \omega_1 = \omega_{n1}, \quad \omega_2 = \omega_{n2} \quad \text{and} \quad \omega_3 = \omega_{n3} \tag{14}$$

where ω is the driving frequency of the muscles and ω_n is the natural frequency of the primary system.

3.2 Passive control systems

Gebai et al. (2018) proposed five different dynamics DVAs. In this paper, we investigated two absorbers inspired by his work. The DVAs are attached to the primary system aiming to control undesired vibration. The total mass of dual parallel absorbers and triple parallel absorbers have the same total mass that is $0.44751\ kg$.

The dual parallel conventional absorber (DPA) combines two similar devices (DVA). The first device is tuned at the first natural frequency of the primary system, and the second at the second natural frequency. The triple parallel absorber combines three similar devices. The first two absorbers are tuned at the same frequency of the DPA, and the third device is tuned at the third natural frequency of the primary system. The dual parallel absorber is attached to the forearm at $l_{a_1} = 0.27\ m$ and $l_{a_2} = 0.29\ m$ from the elbow. However, the triple parallel absorber is attached to two different limbs: the first device is located at the upper arm ($l_{ab_1} = 0.36\ m$ from the shoulder), the other two devices are to the forearm $l_{ab_2} = 0.27\ m$ and $l_{ab_3} = 0.29\ m$ from the elbow. These values were chosen to potentialize the absorption of undesired vibration even more for working closely at the vibration source. Passive controls configurations attached to a primary system are Fig. 3 (a) dual parallel conventional tuned mass damper (DPA), (b) triple parallel conventional tuned mass damper (TPA).

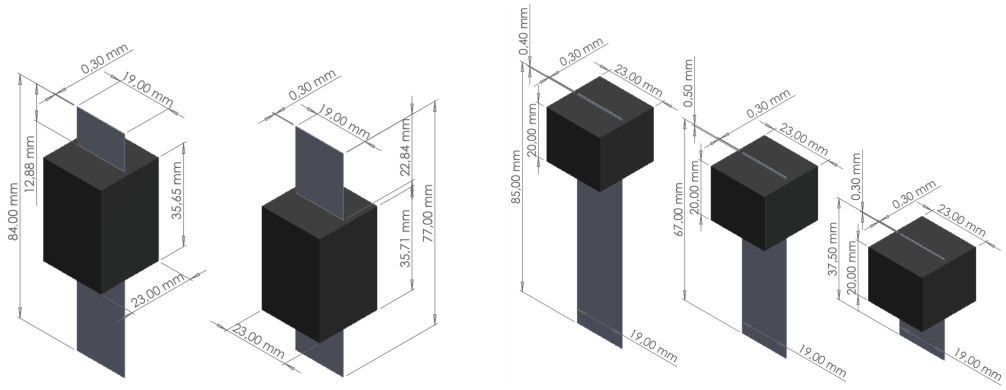

(a) (b)

Figure 3: Passive controllers modeled as cantilevered beam with attached proof mass: (a) DPA and (b) TPA.

In this case, the equation of motion for the primary system within the controls follows the same steps as the primary system. By using the DPA on the primary system, the matrices yield:

$$\mathbf{M} = \begin{bmatrix} M_{11} & M_{12} & M_{13} & M_{14} & M_{15} \\ M_{21} & M_{22} & M_{23} & M_{24} & M_{25} \\ M_{31} & M_{32} & M_{33} & M_{34} & M_{35} \\ M_{41} & M_{42} & M_{43} & M_{44} & M_{45} \\ M_{51} & M_{52} & M_{53} & M_{54} & M_{55} \end{bmatrix} \tag{15}$$

where

$$\begin{aligned}
M_{11} &= (I_1 + m_1 a_1^2) + (I_2 + m_2 a_2^2) + m_2 l_1^2 + I_3 + m_3(l_1^2 + l_2^2 + a_3^2 + 2l_2 a_3) + m_{b_1}(l_1^2 + a_{b1}^2) \\
&\quad + m_{b_2}(l_1^2 + a_{b2}^2) + m_{ab_1}(l_1^2 + a_{b1}^2 + l_{ab_1}^2 + 2a_{b1} l_{ab_1}) + m_{ab_2}(l_1^2 + a_{b2}^2 + l_{ab_2}^2 + 2a_{b2} l_{ab_2}) \\
M_{12} &= (I_2 + m_2 a_2^2) + I_3 + m_3(l_2^2 + a_3^2 + 2l_2 a_3) + m_{b_1} a_{b1}^2 + m_{b_2} a_{b2}^2 + m_{ab_1}(l_{ab_1}^2 + a_{b1}^2 + 2l_{ab_1} a_{b1}^2) \\
&\quad + m_{ab_2}(l_{ab_2}^2 + a_{b2}^2 + 2l_{ab_2} a_{b2}^2) \\
M_{13} &= I_3 + m_3(a_3^2 + l_2 a_3) \\
M_{14} &= m_{ab_1}(l_{ab_1}^2 + l_{ab_1} a_{b1}) \\
M_{15} &= m_{ab_2}(l_{ab_2}^2 + l_{ab_2} a_{b2}) \\
M_{21} &= M_{12} \quad M_{22} = M_{12} \quad M_{23} = M_{13} \quad M_{24} = M_{14} \quad M_{25} = M_{15} \\
M_{31} &= M_{13} \quad M_{32} = M_{23} \quad M_{33} = I_3 + m_3 a_3^2 \quad M_{34} = 0 \quad M_{35} = 0 \\
M_{41} &= M_{14} \quad M_{42} = M_{24} \quad M_{43} = M_{34} \quad M_{44} = m_{ab_1} l_{ab_1}^2 \quad M_{45} = 0 \\
M_{51} &= M_{15} \quad M_{52} = M_{25} \quad M_{53} = M_{34} \quad M_{54} = M_{45} \quad M_{55} = m_{ab_2} l_{ab_2}^2
\end{aligned}$$

$$\mathbf{K} = \begin{bmatrix} k_1 + k_3 & k_3 & 0 & 0 & 0 \\ k_3 & k_2 + k_3 & 0 & 0 & 0 \\ 0 & 0 & k_4 & 0 & 0 \\ 0 & 0 & 0 & k_{a_1} & 0 \\ 0 & 0 & 0 & 0 & k_{a_2} \end{bmatrix} \tag{16}$$

and

$$\mathbf{C} = \begin{bmatrix} c_1 + c_3 & c_3 & 0 & 0 & 0 \\ c_3 & c_2 + c_3 & 0 & 0 & 0 \\ 0 & 0 & c_4 & 0 & 0 \\ 0 & 0 & 0 & c_{a_1} & 0 \\ 0 & 0 & 0 & 0 & c_{a_2} \end{bmatrix} \tag{17}$$

3.3 Absorber design

The absorber design consist of a beam attached to a mass on the free tip as showing in Fig. 3 (Gebai et al., 2016b). The dimension of each absorber is displayed on Table 4.

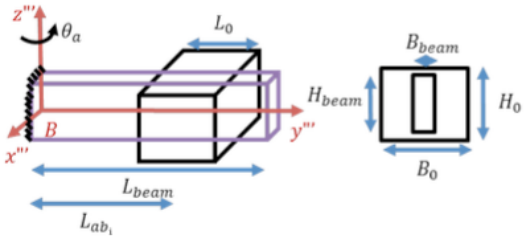

Figure 4: Designed dynamic vibration absorber (Gebai et al., 2016b).

Table 4: Dimensions of the DPA system Gebai et al. (2018)

Absorber	Components	L (cm)	H (cm)	B (cm)
DPA-SA1	Beam	8.4	1.9	0.03
	Attached Mass	3.56	2.3	2.3
DPA-SA2	Beam	7.7	1.9	0.03
	Attached Mass	3.57	2.3	2.3
TPA-SA1	Beam	8.5	1.9	0.03
	Attached Mass	2	2.3	2.3
TPA-SA2	Beam	6.7	1.9	0.03
	Attached Mass	2	2.3	2.3
TPA-SA3	Beam	3.75	1.9	0.03
	Attached Mass	2	2.3	2.3

The position of the copper mass in each absorber was calculated following the Dunkerley's semi-empirical formulation which gives a lower band approximation (Jeffcott, 1918) to satisfy the frequency tuning condition

$$\frac{1}{\omega_{a_i}^2} \simeq \frac{1}{\omega_{beam}^2} + \frac{1}{\omega_{m_0}^2}, \quad i = \{1, 2, 3\} \tag{18}$$

where

$$\omega_{beam} = 3.5160\sqrt{\frac{E_{beam} I_{beam}}{m_{beam} L_{beam}^3}} \tag{19}$$

$$\omega_{m_0} = \sqrt{\frac{6 E_{beam} I_{beam}}{m_{a_i} a_i^2 (3L_{beam} - a_i)}}, \quad i = \{1, 2, 3\} \tag{20}$$

by following (Gebai et al., 2016b), the parameters are $E_{beam} = 189.6\ GPa$, $\rho_{beam} = 7800\ kg/m^3$, and $\rho_{m_{a_i}} = 8900\ kg/m^3$. Thus, the DPA the positions assumed by each absorber are

$$l_{ab_1} = 0.0533\ m \quad and \quad l_{ab_2} = 0.0363\ m$$

In the TPA the positions assumed by each absorber are

$$l_{ab_1} = 0.0746\ m, \quad l_{ab_2} = 0.0565\ m \quad and \quad l_{ab_3} = 0.0272\ m$$

The stiffness (k_{a_i}) and damping (c_{a_i}) coefficients are assumed to be proportional by a constant (Hashemi et al., 2004), such that $c_{a_i} = 0.005\ k_{a_i}\ Nms/rd$, $i = \{1, 2, 3\}$, chosen to match the selected tuning frequency the system. The absorbers are designed to satisfy the loci frequency of $A_{1_{ij}}$. The dynamic response is obtained using the transfer function ($H(\omega) = \{(-\omega^2\mathbf{M} + \mathbf{K}) + i\omega\mathbf{C}\}^{-1}$) of the coupled system. The frequency domain response (θ) is obtained using the receptance transfer function (α) as follows (Gebai et al., 2016c):

$$\alpha_k = \begin{Bmatrix} \frac{A_{1_{ij}} + jB_{1_{ij}}}{A_2 + jB_2} \\ \cdot \\ \cdot \\ \cdot \\ \frac{A_{1_{nj}} + jB_{1_{nj}}}{A_2 + jB_2} \end{Bmatrix} = \begin{Bmatrix} \frac{\theta_{ij}}{F_j} \\ \cdot \\ \cdot \\ \cdot \\ \frac{\theta_{nj}}{F_j} \end{Bmatrix} \tag{21}$$

and the amplitude of angular displacement as

$$\theta_{ij} = \sum_{j=1}^{n} |\alpha_j| F_j \tag{22}$$

where i, j are the i-th row and j-th column for the $n \times n$ transfer function of the n-DOF system. Controllers tuned to the wrist joint's response due to shoulder muscle activation must satisfy the following condition $A_{1_{31}} = 0$, $A_{1_{32}} = 0$ and $A_{1_{33}} = 0$. Hence, the stiffness of each absorber can be determined as shown in Table 5, in addition to the absorbers mass.

Table 5: The stiffness of absorbers

Works	DPA-SA1 (Nm/rd)	DPA-SA2 (Nm/rd)	TPA-SA1 (Nm/rd)	TPA-SA2 (Nm/rd)	TPA-SA3 (Nm/rd)
In present work	0.242	0.2454	0.2664	0.3332	0.4609

Thereupon, we can simulate the respective absorbers from the parameters that satisfy the tuning conditions to evaluate their efficiency in tremor suppression.

4. RESULTS AND DISCUSSIONS

The natural frequency of each system mentioned in previews section is calculated by solving eigenvalue problems (Meirovitch, 2000). Table 6 gathers the frequencies for the hand and arm model without control and controlled by absorbers DPA and TPA. All frequency values follow the refereed paper except for the DPA last frequency, which presents an error of 28%.

Table 6: The natural frequencies of hand arm model

System	ω_{n1} (Hz)	ω_{n2} (Hz)	ω_{n3} (Hz)	ω_{n4} (Hz)	ω_{n5} (Hz)	ω_{n6} (Hz)
No control	3.5880	5.3010	14.34746			
DPA	3.2818	3.6244	4.8060	5.6709	14.26314	
TPA	3.4056	3.6027	5.0541	5.3666	11.7744	15.7094

The position of each absorber in the forearm influences the tremor attenuation. In this paper, in the DPA, the distance placed SA1 is $ab_2 = 0.27\ m$ and SA2 is $ab_3 = 0.29\ m$ from the elbow joint. On the other hand, in the TPA, the distance placed SA1 is $ab_1 = 0.36\ m$ from the shoulder joint, SA2 is $ab_2 = 0.27\ m$ and SA3 is $ab_2 = 0.29\ m$ from. Gebai attached the majority of the absorbers at the same position on the forearm, which are far $0.085\ m$ from the wrist joint ($l_a = l_2 - 0.085$), decreasing the natural frequencies of the systems within DVAs.

Graphs of figures 5, 6 and 7 show the system's behaviour in the frequency and time domains. A harmonic excitation expressed in Eq. (14) is input at the shoulder joint, where each excitation frequency corresponds to the first limb natural frequencies. The results also demonstrate shoulder, biceps, elbow and wrist muscle activation dynamic response.

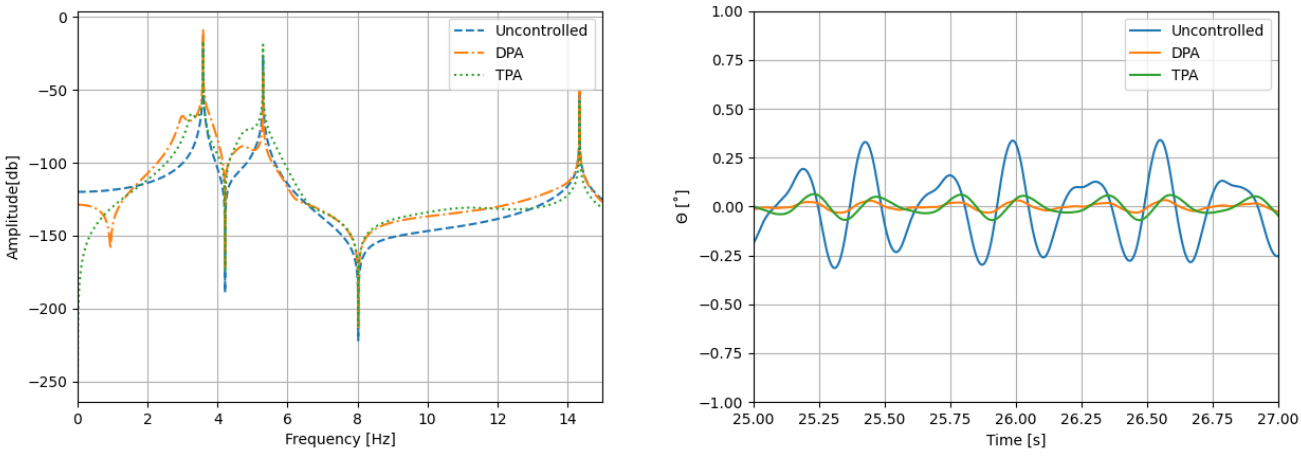

(a) (b)

Figure 5: **Frequency domain response (a) and time domain response (b) at the shoulder joint.**

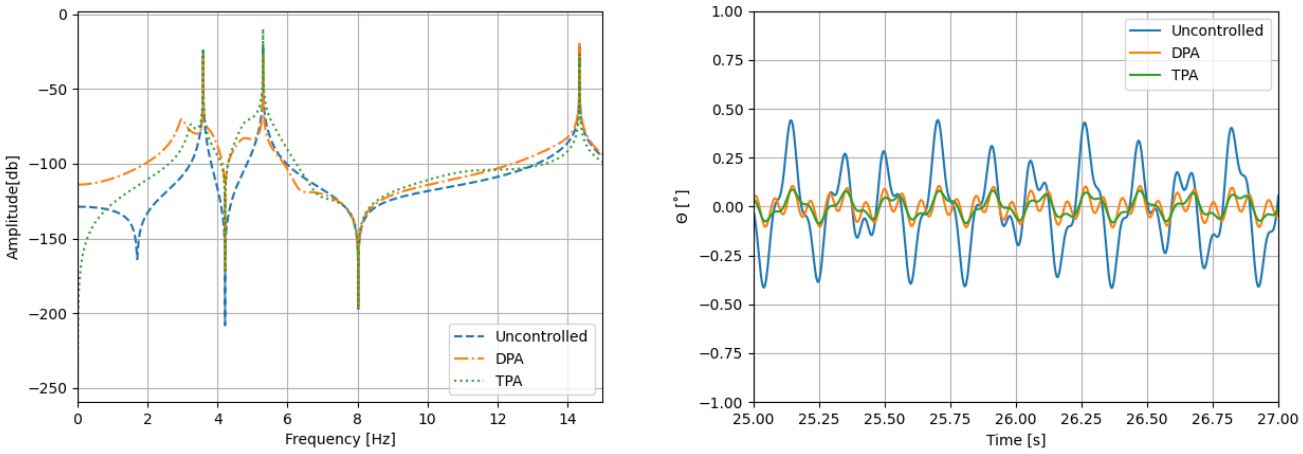

(a) (b)

Figure 6: **Frequency domain response (a) and time domain response (b) at the elbow joint.**

Figure 5a shows the frequency response function (FRF) obtained at the shoulder joint for the upper limb without control (blue dashed line) and controller using DPA (orange line), and TPA (green line). The absorbers have designed values for each driving frequency to control the tremor. All absorbers can significantly reduce the resonant frequency magnitude. DPAs induced resonant frequencies in some bandwidths but presented a good control at the tuned frequency. It shows that the absorber can reduce the tremor's amplitude around the tuning frequency. Figure 6a and Figure 7a shows the FRF obtained at the elbow and wrist joints, with and without control, respectively. A similar analysis applied to those two joints shows the controllers performing approximate attenuation of the shoulder.

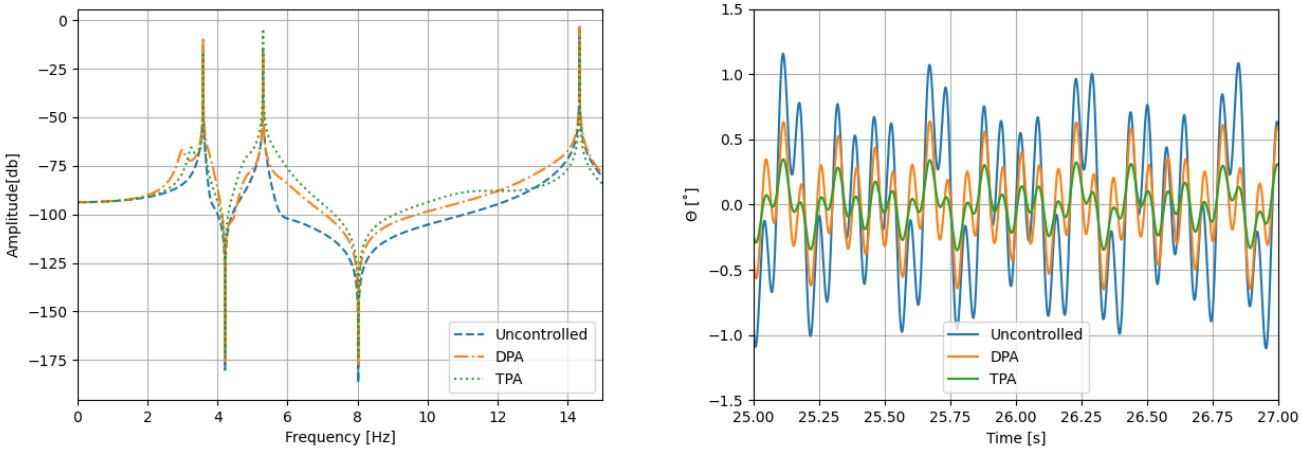

(a) (b)

Figure 7: **Frequency domain response (a) and time domain response (b) at the wrist joint.**

The temporal angular displacement of shoulder joint is showing Fig. 5b, elbow joint in Fig. 6b and wrist joints in Fig. 7b. The highest reduction at the wrist joint is provided by the system controlled by the triple parallel absorber compared to the dual parallel absorber. The DVAs have suppressed the amplitude of the primary system that can be estimated as the reduction percentage calculated by (Gebai et al., 2018):

$$Max.(\%\ Red.) = \frac{max.(\theta_{uncontrolled}) - max.(\theta_{controlled})}{max.(\theta_{uncontrolled})} \times 100 \tag{23}$$

The percentage of amplitude reduction at the shoulder, elbow and wrist joints due to the dual and triple controllers is presented in Table 7. All those results were calculated using the particular solution, given that the homogeneous response in range from 0 to 15 seconds, approximately.

Table 7: Percentage reduction in tremor's amplitude

Absorbers	Shoulder joint (%)	Elbow joint (%)	Wrist joint (%)
DPA	90.14	75.30	50.05
TPA	79.82	79.64	72.85

In comparison between DPA and TPA, the dual parallel absorber is the best range of percentage reduction in the shoulder. At the elbow joint, both absorbers exhibit a similar reduction percentage, although the TPA outperforms the DPA. However, the TPA makes the highest reduction at wrist joint which can reduce the tremor to $72.85\ \%$, it differs by approximately 22.8% from the DPA. The DPA and TPA were efficient controllers showing a good percentage reduction operating at a wide frequency band. Therefore, compared to uncontrolled ones, the controlled system shows a great decrease in amplitude in both time and frequency domain responses at the joints.

5. CONCLUSION AND FUTURE WORK

This paper intends to study and test the best configuration of absorbers in suppressing the tremor derived from Parkinson's patients. The responses of the uncontrolled and controlled structures are compared in the frequency and time domains. The efficiency of each controller was analyzed in terms of response magnitude and percentage of amplitude reduction. Indeed, the distance along the forearm measured from the elbow joint can significantly decrease the response amplitude if it is placed near the elbow joint. It is known that palm vibration is the symptom with the most significant negative impact on the patient's quality of life, the TPA is demonstrated as the most effective controller presented in this work, resulting in a substantial reduction in wrist joint amplitude and improved weight distribution. The effect of more than two absorbers in parallel along the forearm can be analyzed and compared to the present TPA, after evidence of effectiveness in reducing the angular motion at the wrist joint. Hence, it can improve our knowledge of devices as well as guide us for new absorbers design applied to control human limb tremors.

6. ACKNOWLEDGEMENTS

The author appreciate the supports from Fundação de Apoio a Pesquisa do Distrito Federal-FAPDF (Grants no. 00193-00000766/2021-71 and 00193- 00000826/2021-55)

7. REFERENCES

Paul F Crawford III and Ethan E Zimmerman. Tremor: sorting through the differential diagnosis. *American family physician*, 97(3):180–186, 2018.

Kelvin L Chou. Diagnosis and management of the patient with tremor. *Rhode Island Medical Journal*, 87(5):135, 2004.

S Morrison, Graham Kerr, and Peter Silburn. Bilateral tremor relations in parkinson's disease: Effects of mechanical coupling and medication. *Parkinsonism & related disorders*, 14(4):298–308, 2008.

Nancy L Diaz and Elan D Louis. Survey of medication usage patterns among essential tremor patients: movement disorder specialists vs. general neurologists. *Parkinsonism & related disorders*, 16(9):604–607, 2010.

Nicolas Philip Fromme, Martin Camenzind, Robert Riener, and René Michel Rossi. Need for mechanically and ergonomically enhanced tremor-suppression orthoses for the upper limb: a systematic review. *Journal of neuroengineering and rehabilitation*, 16(1):1–15, 2019.

SM Hashemi, MF Golnaraghi, and AE Patla. Tuned vibration absorber for suppression of rest tremor in parkinson's disease. *Medical and Biological Engineering and Computing*, 42(1):61–70, 2004.

Sarah Gebai, Mohamad Hammoud, Ali Hallal, Ali Al Shaer, and Hassan Khachfe. Passive vibration absorber for tremor in hand of parkinsonian patients: Tuned vibration absorber for rest tremor. In *2016 3rd International Conference on Advances in Computational Tools for Engineering Applications (ACTEA)*, pages 162–167, 2016a. doi: 10.1109/ACTEA.2016.7560132.

GGSB Albuquerque, MR Machado, and BB Moura. Comparison of passive dynamic absorbers in attenuating pathological tremor of human upper limb: an analytical approach. *DINAME 2023 XIX International Symposium on Dynamic Problems of Mechanics*, 2023.

Seyedeh Marzieh Hosseini, Hamed Kalhori, and Adel Al-Jumaily. Active vibration control in human forearm model using paired piezoelectric sensor and actuator. *Journal of Vibration and Control*, 27(19-20):2231–2242, 2021.

Sarah Gebai, Mohammad Hammoud, Ali Hallal, and Ali Al Shaer. Structural control and biomechanical tremor suppression: Comparison between different types of passive absorber. *Journal of Vibration and Control*, 24(12):2576–2590, 2018.

Renato Contini. Body segment parameters, part ii. *Artificial limbs*, 16(1):1–19, 1972.

Sarah Gebai, Mohammad Hammoud, Ali Hallal, and Hassan Khachfe. Tremor reduction at the palm of a parkinson's

patient using dynamic vibration absorber. *Bioengineering*, 3(3):18, 2016b.

HH Jeffcott. The periods of lateral vibration of loaded shafts.—the rational derivation of dunkerley's empirical rule for determining whirling speeds. *Proceedings of the Royal Society of London. Series A, Containing Papers of a Mathematical and Physical Character*, 95(666):106–115, 1918.

Sarah Gebai, Mohamad Hammoud, and Hassan Khachfe. Using a dual vibration absorber to suppress rest hand tremor of elderly. In *The Fifth International Conference on Global Health Challenges, GLOBAL HEALTH*, 2016c.

L Meirovitch. Fundamentals of vibrations/meirovitch, l, 2000.

8. RESPONSIBILITY NOTICE

The author(s) is (are) the only responsible for the printed material included in this paper.